



Cite this: *Food Funct.*, 2020, **11**, 8051

## Sacha inchi (*Plukenetia volubilis* L.) shell extract alleviates hypertension in association with the regulation of gut microbiota<sup>†</sup>

Pan Li,<sup>a</sup> Xin Cai,<sup>a</sup> Nan Xiao,<sup>a</sup> Xiaowei Ma,<sup>a</sup> Liping Zeng,<sup>a</sup> Lian-Hui Zhang,<sup>\*b</sup>  
Lanhua Xie<sup>c</sup> and Bing Du  <sup>\*a,c</sup>

Dysbiosis of gut microbiota has been implicated in the pathogenesis of hypertension. A definite relationship between gut microbiota and hypertension remains intriguing. Here, we show that the Sacha inchi (*Plukenetia volubilis* L.) shell extract (SISE) intervention significantly reduced systolic blood pressures in spontaneous hypertensive rats (SHR), attenuated the oxidative damage and modulated plasma calcium homeostasis and left ventricular hypertrophy in both SHR and high-salt diet Wistar-Kyoto rats. SISE reshaped the gut microbiome and metabolome, particularly by improving the prevalence of *Roseburia* and dihydrofolic acid levels in the gut. Transcriptome analyses showed that the protective effects of SISE were accompanied by the modulation of renal molecular pathways, beneficial for cardiovascular functions such as the L-type voltage-dependent calcium channel (LTCC), a key regulator of calcium signaling. Overall, the results have shown that dietary SISE can alleviate hypertension regulating the gut microbiota, and Ca<sup>2+</sup> signaling might be a potential target for spontaneous hypertension.

Received 7th July 2020,  
Accepted 7th August 2020

DOI: 10.1039/d0fo01770a

rsc.li/food-function

## 1. Introduction

Hypertension is one of the most common causes of prevalent cardiovascular diseases worldwide, including stroke, heart failure, and myocardial infarction.<sup>1</sup> The pathogenesis of hypertension is very complex and lifestyle factors, such as diet, are important drivers of the disease.<sup>2</sup> Recently, several lines of evidence have suggested the link between gut microbiota dysbiosis and hypertension. It has been reported that high salt intake can lead to hypertension and cardiovascular diseases affecting the gut microbiota in mice, particularly, leading to the depletion of *Lactobacillus murinus*, and consequently, treatment of mice with *L. murinus* prevents salt-sensitive hypertension.<sup>3,4</sup> In addition, significant decrease in microbial richness and diversity were observed in spontaneously hypertensive rats.<sup>5</sup> Significantly, fecal transplantation from hypertensive human donors to germ-free mice led to an elevated

blood pressure indicating the direct influence of gut microbiota on the host blood pressure.<sup>6</sup> While these findings are encouraging, it is far from clear on how dysbiosis could lead to onset of hypertension and cardiovascular diseases.

Several treatments, including antihypertensive drugs, probiotics, and prebiotics have been evaluated for the management of hypertension. For example, the treatment of spontaneous hypertensive rats with probiotic *Lactobacillus* could exert cardiovascular protective effects with improved vascular pro-oxidative and -inflammatory status.<sup>7</sup> In addition, the excess consumption of high-fiber diet could attenuate the development of hypertension with increased prevalence of acetate-producing bacteria, thereby, improving the levels of *Bacteroides acidifaciens*, and decreasing gut dysbiosis.<sup>8</sup> The gut microbiota is thus considered a new territory for potential drug targeting. For instance, the drug metformin, which is used to treat type 2 diabetes by regulating the upper small intestinal sodium-glucose cotransporter-1, changes the composition of the microbiota with increased abundance of *Lactobacillus*,<sup>9</sup> but its effect on hypertension has not yet been described. Additionally, the treatment of rats with antibiotic ampicillin might increase the bioavailability of amlodipine by suppressing gut microbial metabolic activities.<sup>10</sup> Since amlodipine is a calcium channel blocker frequently used for the treatment of hypertension,<sup>10</sup> the prevention of over metabolism would help to improve its pharmaceutical effect. However, the side effects of antibiotics on beneficial micro-organisms

<sup>a</sup>College of Food Science, South China Agricultural University, Guangzhou 510642, China

<sup>b</sup>Guangdong Province Key Laboratory of Microbial Signals and Disease Control, Integrative Microbiology Research Centre, South China Agricultural University, Guangzhou 510642, China. E-mail: Lhzheng01@scau.edu.cn

<sup>c</sup>Expert Research Station of Bing Du, Pu'er City, Yunnan, 665000, China.  
E-mail: dubing@scau.edu.cn; Fax: +020-85283592; Tel: +86-13929522370

<sup>†</sup>Electronic supplementary information (ESI) available. See DOI: 10.1039/d0fo01770a

remain a serious concern. These findings highlight the potential of using biotic or chemical intervention approaches to modulate gut microbiota in the treatment of hypertension, and emphasize the need to search for potent and reliable drugs for the management of gut microbiota and hypertension.

Sacha inchi (*Plukenetia volubilis* L.) is an oleaginous plant that belongs to the Euphorbiaceae family.<sup>11</sup> It grows in the rain forests of the Andean region in South America and in several South East Asiatic countries, such as China. The Sacha inchi shell (SIS) is traditionally used as an important source of phytochemicals, especially polysaccharides and polyphenols.<sup>12</sup> In our preliminary experiment, we found that the Sacha inchi shell water extract (SISE) could effectively inhibit the angiotensin-converting enzyme (ACE) activity and decrease the blood pressure of spontaneously hypertensive rats (SHR).<sup>13</sup> Given that hypertension is linked to gut dysbiosis and pathological changes,<sup>3,5,14,15</sup> and that captopril, an ACE inhibitor, can normalize blood pressure and reverse gut pathology,<sup>15</sup> we, therefore, hypothesized that SISE administration might inhibit the progression of hypertension through the regulation of gut microbiota.

Previous work has shed light on the potential mechanisms by which the gut microbiota and its metabolites, including short-chain fatty acids, trimethylamine N-oxide, and lipopolysaccharides, act on downstream cellular targets to prevent or contribute to the development of hypertension.<sup>2,16,17</sup> However, a definite relationship between the gut microbiota and hypertension remains intriguing. RNA-sequencing (RNA-seq) has been widely used in transcriptome analysis to identify differentially expressed genes and to elucidate the more complex signaling pathways involved in the pathogenesis of chronic metabolic diseases.<sup>18,19</sup> In the present study, we have shown that SISE intervention exerts a significant influence on systolic blood pressures, gut microbiome and metabolome in both SHR and high-salt diet Wistar-Kyoto (WKY) rats. We performed RNA-seq to explore the role of SISE in the renal transcriptome and found that the protective effects of SISE were also associated with the modulation of renal molecular pathways beneficial for cardiovascular functions.

## 2. Materials & methods

### 2.1. Animals

Ten male SHR rats (8 weeks of age, body weight ~210–230 g) and twenty-eight male WKY rats (8 weeks of age, body weight ~195–225 g) were provided,<sup>7,20</sup> bred, and housed individually in Guangdong Medical Laboratory Animal Center (Foshan, Guangdong, China, certification no. SYXK-<Guangdong>-2013-0002), and maintained in a controlled environment (12 h day-light cycle, lights off at 18:00) with food and water *ad libitum*.

### 2.2. Ethics statement

All experimental protocols were approved by and performed at the Animal and Ethics Review Committee of Guangdong

Medical Laboratory Animal Center (Foshan, China) according to the National Guidelines for Experimental Animal Welfare (Ministry of Science and Technology of the People's Republic of China, 2006).

### 2.3. SISE intervention

The SIS materials were collected from Puer U-Multitude Biological Resources Co. Ltd (Puer, Yunnan Province, China), boiled in water (1:40, w/v) for 3 h, and then lyophilized to obtain the SISE sample. The composition of SISE was analyzed, and the major components were identified according to previous reports.<sup>11,21</sup> SISE consists of 37.86 ± 0.27% fiber, 22.74% ± 0.27% soluble sugars, 12.46% ± 0.08% polysaccharides, 14.52% ± 0.21% polyphenols, 0.35% ± 0.06% saponins, and 1.83% ± 0.06% flavonoids. After 2 weeks of acclimation on a standard pellet diet (Guangdong Medical Laboratory Animal Center, Foshan, China; containing 16 kcal% casein protein, 51 kcal% carbohydrates, 3 kcal% fats, and a variety of essential vitamins and trace elements), the SHR and WKY rats were randomly divided into the following treatment groups. SHR (normal diet, administration of water [10 mL kg<sup>-1</sup>], as the SHR control group; *n* = 5); SHR + SISE (normal diet, oral administration of 400 mg kg<sup>-1</sup> d<sup>-1</sup> SISE [10 mL kg<sup>-1</sup>]; *n* = 5); WKY (normal diet, oral administration of water [10 mL kg<sup>-1</sup>] as the WKY control group; *n* = 6); WKY + SISE (normal diet, oral administration of 400 mg kg<sup>-1</sup> d<sup>-1</sup> SISE [10 mL kg<sup>-1</sup>]; *n* = 5); WKY + SA (high-salt diet, oral administration of water [10 mL kg<sup>-1</sup>]; *n* = 8); WKY + SA + SISE (high-salt diet, oral administration of 400 mg kg<sup>-1</sup> d<sup>-1</sup> SISE [10 mL kg<sup>-1</sup>]; *n* = 9). The high-salt diet was identical in composition to the normal diet, except that it contained 4% NaCl.<sup>3</sup> The animals were monitored and weighed regularly throughout the experiment. Systolic blood pressure (SBP) was measured at room temperature using tail-cuff plethysmography as described previously.<sup>7</sup> After the experimental period, the rats were anesthetized with 2.5 mL kg<sup>-1</sup> equitansin (i.p.), and blood was collected from the abdominal aorta. Stool samples were collected steriley from the colon, and the heart (divided into right and left ventricles) and kidney tissues were rapidly removed, weighed, and immediately flash-frozen in liquid nitrogen, and stored at -80 °C for subsequent analyses.

### 2.4. Histological and biochemical analyses

Heart and kidney tissues were fixed in 10% buffered formalin, paraffin-embedded, cut into 6 µm sections, stained with haematoxylin and eosin, and examined under an Olympus BH2 microscope. The ventricular wall thickness was quantified using the ImagePro Plus software (Adept Electronic Solutions Pty Ltd, Moorabbin, Australia) by measuring the distance from the inner to the outer myocardial edges at the mid-chamber zone. Plasma Ca<sup>2+</sup> was estimated immediately by using an automated electrolyte analyzer (FT-1000 Automatic Chemical Analyzer, Fortune company Limited, Chengdu, China), and the contents of plasma Na<sup>+</sup>, nitric oxide (NO), superoxide dismutase (SOD), glutathione (GSH) and malondialdehyde (MDA)

were estimated by reagent kits (NanJing JianCheng Bio Inst, Nanjing, China).

## 2.5. Gut microbiome

DNA was extracted from stool samples using a faecal DNA isolation kit (MoBio Laboratories, USA), and the V4 region of the bacterial 16S rRNA was sequenced with the 515F and 806R primers in an Illumina MiSeq sequencer (300 bp paired-end reads).<sup>22</sup> After filtration and chimera removal, the clean sequence was finally obtained. UPARSE software (UPARSE v7.0.1001) was used to obtain operational taxonomic units (OTUs) with 97% sequence similarity.<sup>23</sup> Representative sequences were picked for each OTU, and the Silva database was used to annotate the taxonomic information based on the Mothur algorithm. Alpha diversity indices, beta diversity on a weighted Unifrac distance, and the ANOSIM test for significance were calculated within QIIME.<sup>24</sup> Non-metric multidimensional scaling (NMDS) and principal component analysis (PCA) were visualized based on OTUs using R software (v2.15.3). Linear discriminant analysis effect size (LEfSe) analysis was performed using the Galaxy platform at a  $P < 0.05$ , LDA score  $>3.0$ .<sup>25</sup>

## 2.6. Untargeted gut microbiota metabolomic analysis

All stool samples (0.1 g) were homogenized with 500  $\mu$ L of methanol at 4 °C. The samples were vortexed for 1 min, ultrasonicated for 1 min, and vortexed once more for 1 min prior to centrifugation at 12 000 rpm for 15 min at 4 °C; 200  $\mu$ L of supernatant was transferred to a vial for analysis. The untargeted metabolomic analysis was performed on a Vanquish UHPLC system (Thermo Fisher) equipped with a Hypergod C18 column (100 × 4.6 mm × 3  $\mu$ m) coupled with an Orbitrap Q Exactive HF-X mass spectrometer (Thermo Fisher). The metabolomic data were processed using the Compound Discoverer 2.0 software (Termo). Compounds were identified by searching *m/z* values against the online Metlin database. Multivariate analyses, including PCA and partial least squares discrimination analysis (PLS-DA), were carried out using the SIMCA-P software (Umetrics AB, Umea, Sweden). The significantly different metabolites between groups were obtained at a variable influence on projection (VIP)  $> 1$ , and  $P$ -value  $<0.05$  based on the peak areas. For metabolites detected in both ES+ and ES- modes, the data in the mode with the higher VIP were retained for further analysis.

## 2.7. Renal transcriptome

RNA extractions from kidney tissues were performed using an RNeasy kit (QIAGEN, Valencia, CA). After DNase treatment and RNA integrity assessment on an Agilent 2100 Bioanalyzer (Agilent Technologies, Waldbronn, Germany), sequencing libraries were generated using the NEBNext® Ultra™ RNA Library Prep Kit for Illumina® (NEB, USA). Index codes were also added to attribute sequences to each sample, as we previously described.<sup>26</sup> The library quality was assessed using the Agilent Bioanalyzer 2100 system, and cluster generation was performed on a cBot Cluster Generation System using the

TruSeq PE Cluster Kit v3-cBot-HS (Illumina) following the manufacturer's instructions. The paired-end sequencing was performed on an Illumina Hiseq platform to yield 150 bp reads. After quality trimming and adapter clipping, read mapping was performed with Hisat2 v2.0.4.<sup>27</sup> The DESeq R package (v1.18.0) was implemented to calculate differential expressions between groups with default parameters.<sup>28</sup> Significance was set to an adjusted  $P$ -value of  $<0.05$  using the Benjamini-Hochberg procedure. Gene Ontology (GO) enrichment analysis of differentially expressed genes was implemented using the GOseq R package,<sup>28</sup> and KOBAS software was used to test the statistical enrichment of differential expression genes in the KEGG pathways.<sup>29</sup>

## 2.8. Correlation analysis

Spearman's correlation coefficients between genera and metabolites, as well as the metabolites and differentially expressed genes, were calculated using R software (v3.2.1) and visualized using the Complex Heatmap package in R software (v3.2.1).  $P$  values were corrected for multiple testing via the Benjamin and Hochberg method. The top 35 genera existing in any of the subjects were considered in the analyses.

## 2.9. Data availability

Raw files of the bacterial V4 16S rRNA data were uploaded to the NCBI Sequence Read Archive as Bioproject PRJNA478341 (SRP151556). Raw files of the renal transcriptome sequencing data were uploaded to the NCBI Sequence Read Archive as Bioproject PRJNA478465 (SRP151693).

## 2.10. Statistical analysis

The sample size of 5 rats was evaluated by a standard deviation of 8.0 at a power of 80% and a significance level of 0.05%. The statistical significance of differences was determined using two-way repeated measures ANOVA followed by Tukey's test with the SPSS 22 software (IBM, Chicago, USA). Differences in the relative abundance of OTUs were calculated using the *T*-test in the R package (v2.15.3). Tukey and Wilcox tests were performed using the R package (v2.15.3) to determine significant differences in alpha and beta diversity indices across groups. The results were considered statistically significant at  $P < 0.05$ .

# 3. Results

## 3.1. SISE intervention decreases SBP and alleviates cardiac hypertrophy

SBP in SHR rats on a normal diet and on a normal diet supplemented with SISE, respectively, were monitored for 51 days. Consistent with previous reports, SBP in the SHR rats increased over the course and they developed hypertension that plateaued between 11 and 13 weeks;<sup>30,31</sup> SHR rats showed exacerbated hypertension that almost plateaued from day 33 as expected (Fig. 1A). Significantly, SISE administration could prevent the further increase of SBP in SHR rats ( $P < 0.05$ ). This

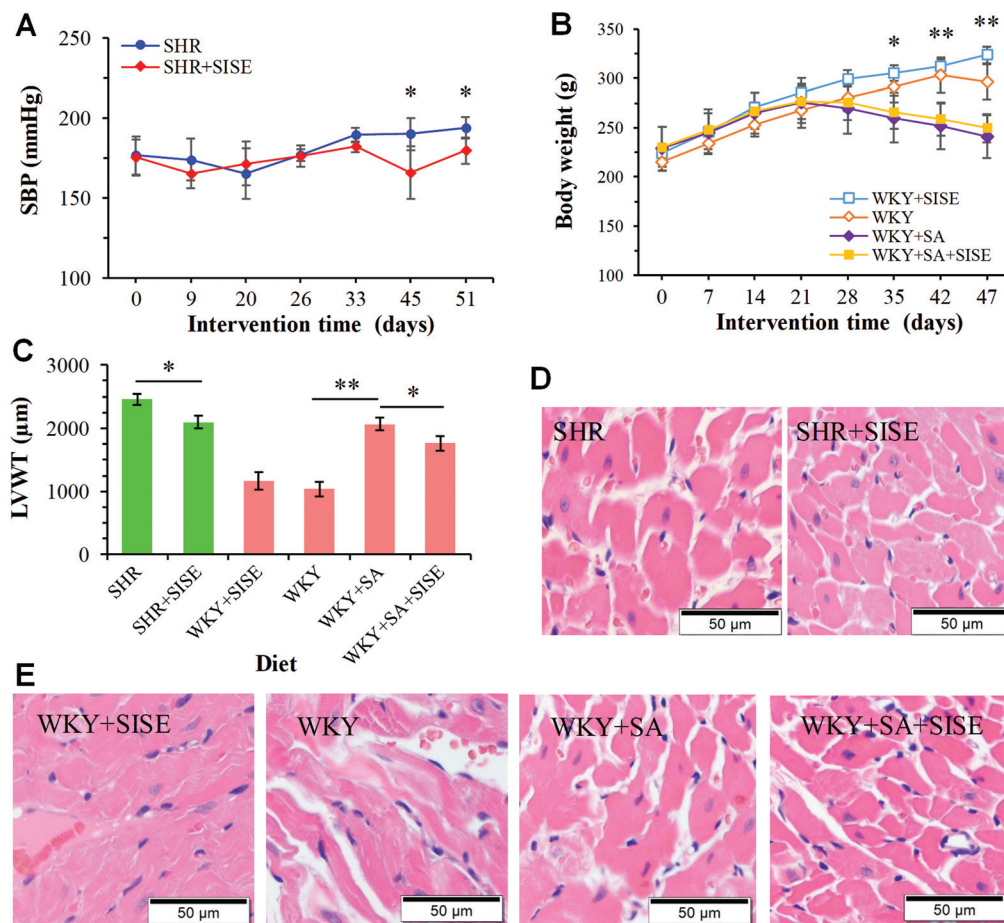


**Fig. 1** The administration of SISE modulates body weight, blood pressure and left ventricular hypertrophy in SHR and WKY rats. SISE administration in SHR rats significantly prevented the increase in SBP (A); high-salt diet in WKY rats led to a reduction in body weight (B); the effects of SISE treatment on LVWT (C) in SHR and WKY rats. Representative histological images of haematoxylin and eosin staining for SISE interventions in SHR (D) and WKY (E) rats. SBP, systolic blood pressure; left ventricular wall thickness, LVWT; \*, P < 0.05; \*\*, P < 0.01.

preventive effect became significant on day 45 ( $190 \pm 10$  mmHg versus  $166 \pm 16$  mmHg,  $P < 0.05$ ; Fig. 1A), and continued to be significant till the completion of the experiment on day 51 ( $194 \pm 7$  mmHg versus  $179 \pm 8$  mmHg,  $P < 0.05$ ; Fig. 1A). The SISE treatment did not affect the weight gain, food and water intake or the ratios of heart/body weight and kidney/body weight (Fig. S1†).

A high intake of salt is associated with an increased risk of hypertension. Unlike the deoxycorticosterone acetate (DOCA)-salt model,<sup>8</sup> the high-salt diet also failed to increase blood pressure in salt-nonsensitive WKY rats,<sup>32,33</sup> but led to a progressive reduction in weight gain and food intake at about 21 days after diet intervention (Fig. S1†), in agreement with previous studies where the high salt diet altered the physiological and behavioral influence of rodents;<sup>34,35</sup> however, SISE intervention could not prevent this reduction (Fig. 1B). Similar to previous reports of SHR rats showing higher left ventricular wall thickness (LVWT) than WKY rats,<sup>36</sup> in the present study, SHR and high-salt diet WKY rats also exhibited much-elevated levels of LVWT as compared with normotensive WKY rats,

which is a common pattern in ventricular hypertrophy and cardiology.<sup>37</sup> Notably, SISE administration could significantly decrease LVWT in both SHR and high-salt diet WKY rats (Fig. 1C). We further conducted the myocardial histology analysis, and the results showed that SISE administration could also ameliorate myocardial interstitial space in SHR and high-salt diet WKY rats (Fig. 1D and E).

### 3.2. SISE intervention attenuates the oxidative damage in SHR and high-salt diet WKY rats

Oxidative stress is a pervasive aspect of cardiovascular disease and occurs whenever the release of reactive oxygen species (ROS) exceeds the endogenous antioxidant capacity.<sup>38</sup> Similar to the previous results of high-salt diet-induced oxidative stress in rats,<sup>39</sup> we found that the high-salt diet elevated the levels of MDA and decreased the levels of NO, GSH, and SOD activity (Fig. 2). In contrast, SISE intervention significantly decreased the levels of MDA and increased the levels of NO, GSH, and SOD activity (Fig. 2). These results indicate that SISE

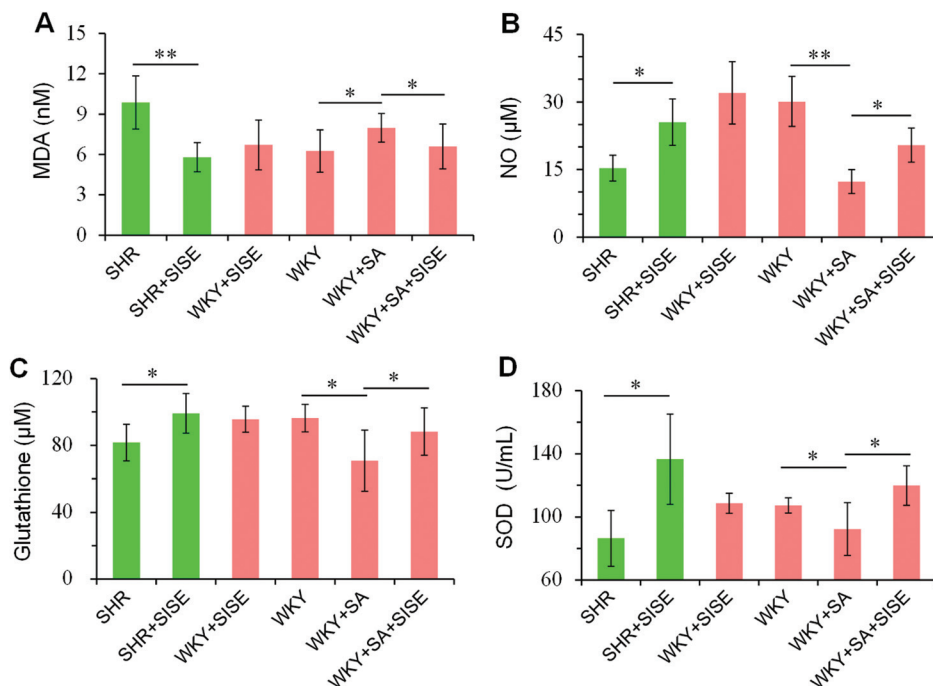


**Fig. 2** SISE intervention attenuates oxidative damage in SHR and high-salt diet WKY rats. The effects of SISE intervention on the plasma levels of MDA (A), NO (B), glutathione (C), and SOD (D) activity in SHR and high-salt diet WKY rats. NO, nitric oxide; MDA, malondialdehyde; SOD, superoxide dismutase. \*,  $P < 0.05$ ; \*\*,  $P < 0.01$ .

intervention can attenuate oxidative damage in both SHR and high-salt diet WKY rats.

### 3.3. SISE intervention alters the gut microbiota of SHR and high-salt diet WKY rats

To examine whether SISE affects the gut microbiota composition in SHR and high-salt diet WKY rats, we sequenced the V4 region of 16S bacterial genes in faecal samples. After selection, a total of 2,455, and 136 clean reads were generated, and each faecal sample produced an average of  $74\,398 \pm 6999$  clean reads. The rarefaction curves approached the saturation plateau, thus indicating that the sequencing depth covered rare phylotypes and most of the diversity in the sample (ESI Fig. S2A†). We also determined the  $\alpha$  and  $\beta$  diversities but SISE intervention did not increase the number of different types of bacteria in the gut (ESI Fig. S2B and C†). Both the non-metric multidimensional scaling (NMDS) and principal component analysis (PCA) revealed distinct clustering of the microbiota composition for each treatment group (Fig. 3A and B). ANOSIM analysis unveiled the statistically significant separation between the microbiota of SHR + SISE and SHR ( $A = 0.212$ ,  $P = 0.118$ ), WKY + SISE and WKY ( $A = 0.315$ ,  $P = 0.016$ ), WKY + SA and WKY ( $A = 0.756$ ,  $P = 0.007$ ), and WKY + SA + SISE and WKY + SA ( $A = 0.494$ ,  $P = 0.002$ ) groups (Fig. 3C). These results indicate that SISE significantly modulated the gut microbiota of SHR, WKY, and high-salt diet WKY rats, the notion was further supported by the difference in the abundance of bacterial phyla between the treatment and control groups (Fig. 3D). We further calculated the ratio of *Firmicutes*

to *Bacteroidetes* (F/B), which is a widely used marker for gut dysbiosis. Notably, a high-salt diet significantly increased the F/B ratio, while SISE intervention reduced and normalized this ratio (Fig. 3E). Interestingly, SHR rats showed an F/B ratio lower than that of the WKY rats, and treatment with SISE significantly elevated the F/B ratio in SHR rats (Fig. 3E).

At the genus level, SISE intervention enhanced the bacterial relative abundances in SHR rats that are negatively correlated with hypertension,<sup>5,14</sup> including *Roseburia* (1.04% versus 0.46%), *Akkermansia* (0.04% versus 0.01%), *Faecalibaculum* (4.73% versus 3.79%), and *Oscillibacter* (1.46% versus 0.46%). However, it decreased the relative abundances of taxa that are frequently distributed in hypertensive gut microbiome,<sup>5,40</sup> such as *Alistipes* (0.46% versus 1.09%), *Parasutterella* (0.15% versus 0.85%), *Bacteroides* (1.57% versus 2.93%), *Parabacteroides* (0.38% versus 0.85%), *Alloprevotella* (6.98% versus 8.38%), *Prevotellaceae* Ga6A1 (0.62% versus 0.68%), *Prevotellaceae* NK3B31 group (0.85% versus 1.92%), and *Prevotellaceae* UCG-001 (0.21% versus 0.82%) (Fig. 3F). Intriguingly, SISE also lowered the relative abundance of *Lactobacillus* (2.23% versus 3.62%) in SHR rats, which was previously reported to reduce blood pressure,<sup>3,7</sup> suggesting that SISE treatment might induce the accretion of other probiotics species associated with blood reduction. The high-salt diet in WKY rats reduced the butyrate-producing *Roseburia* and *Lactobacillus*, but significantly increased the common bacterial species associated with prehypertension or hypertension,<sup>5</sup> such as *Turicibacter*, *Ruminococcus*, *Eubacterium* and the *Prevotellaceae* Ga6A1 group, and the generally considered ben-

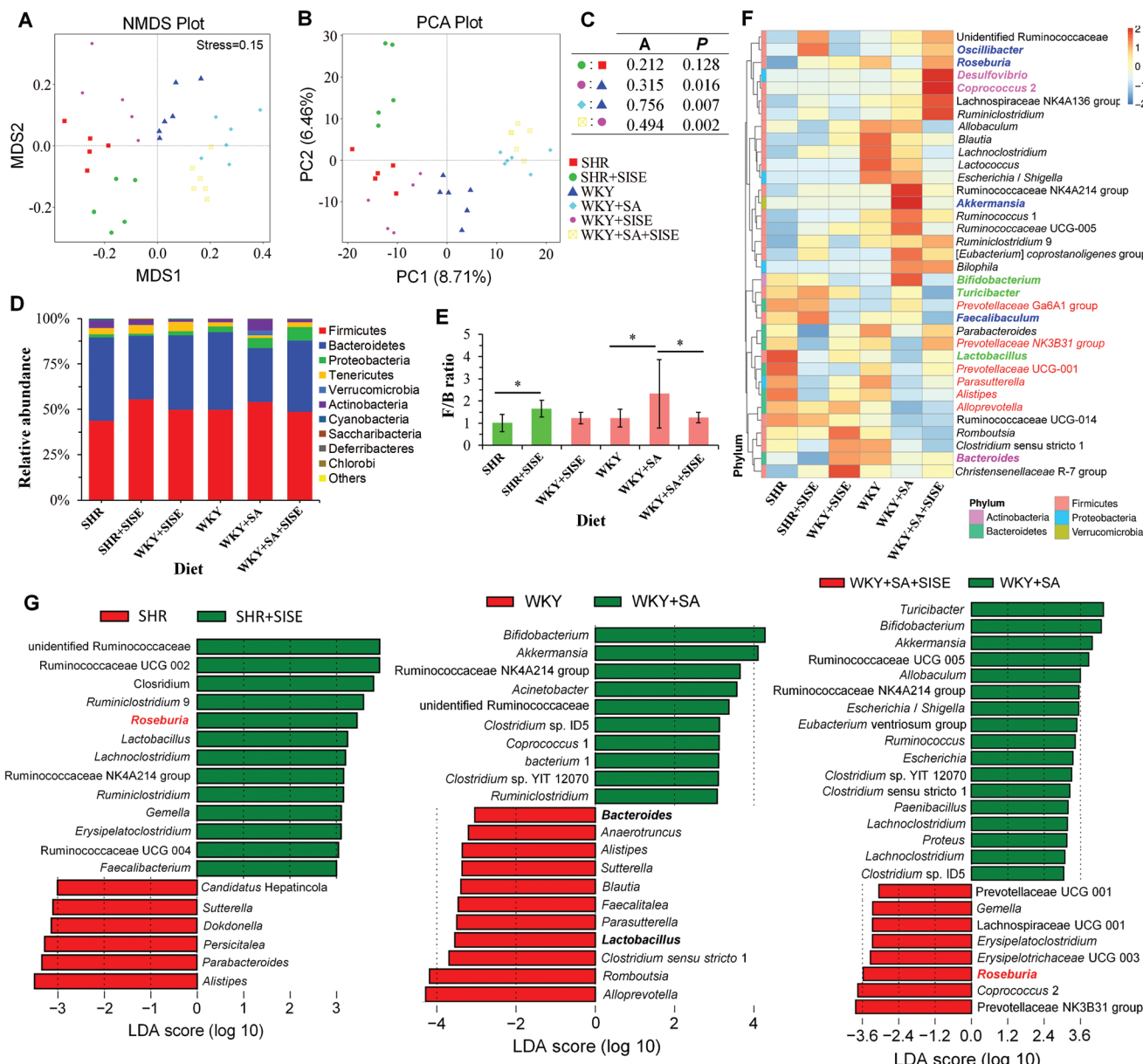


**Fig. 3** SISE intervention alters the gut microbiota of SHR and high-salt diet WKY rats. Non-metric multidimensional scaling (A), principal component analysis (B) and ANOSIM (C) analyses indicate that the composition of the gut microbiota of each group is significantly different;  $A > 0$  means significant differences among treatments,  $P < 0.05$  means statistically significant. The relative percentage of total bacteria presented at the phyla level (D). The Firmicutes to Bacteroidetes (F/B) ratio (E) as a marker of gut dysbiosis; \* represents  $P < 0.05$ . Heatmap of the top 35 genera in each group at the genus level (F); the scale reflects the data as follows: red indicates high values, whereas blue indicates low values for the percentages of reads that were classified at that rank. LEfSe (G) identified the significantly different bacterial taxa enriched in each SHR rat after SISE intervention, high-salt diet WKY rats and high-salt diet WKY rats after SISE intervention, bars represent bacterial taxa.

eficial taxa *Akkermansia* and *Bifidobacterium*, while these effects were reversed and normalized in high-salt diet WKY rats after SISE intervention (Fig. 3F). High-salt diet WKY rats after SISE intervention also enriched *Coprococcus 2* (Fig. 3F), bacteria known to be essential for a healthy status,<sup>5</sup> and *Desulfovibrio*, which is relevant to cardiovascular physiology.<sup>41</sup>

Next, we attempted to distinguish the key phylotypes as microbiological markers at the genus level in each group using linear discriminant analysis effect size (LEfSe). After SISE

intervention, *Roseburia* was enriched in SHR rats (Fig. 3G) and high-salt diet WKY rats (Fig. 3G), and *Faecalibacterium* was also highly accumulated in SHR rats (Fig. 3G). In contrast, *Roseburia* and *Lactobacillus* were mostly diminished, while *Akkermansia* and *Bifidobacterium* were accumulated in the high-salt diet WKY rats (Fig. 3F and G). Therefore, *Roseburia* was the only genus that was maintained at a low level in the control diet but could be highly enriched in both SHR and high-salt diet WKY rats by SISE treatment (Fig. 3F and G).

Collectively, these results show that SISE could reshape the gut microbiota of SHR rats, and ameliorate gut dysbiosis in high-salt diet WKY rats.

### 3.4. SISE intervention affects the gut microbiota metabolome in SHR and high-salt diet WKY rats

To evaluate the effects of SISE on the gut microbiota metabolome, we performed colonic faecal metabolomics by using UHPLC-MS/MS. The PCA of total faecal metabolites showed obvious differences between the treatment and control groups (Fig. 4A). The untargeted UHPLC-MS/MS-based metabolomics analysis detected 220 differentially altered metabolites in SHR rats after SISE intervention, 1667 differentially altered metabolites in high-salt diet WKY rats, and 213 differentially altered metabolites in high-salt diet WKY rats after SISE intervention in comparison with the rats fed the control diet (Fig. 4B and C). The partial least squares discrimination analysis (PLS-DA) also discriminated the metabolic profiles among the groups (Fig. 4D), and validation of this obtained model showed no overfitting phenomenon (ESI Fig. S3†). Collectively, these results showed that SISE intervention altered the gut microbiota metabolome in SHR and high-salt diet WKY rats (ESI Fig. S4†).

Notably, dihydrofolic acid was the only common metabolite differentially enriched by SISE intervention in both SHR and high-salt diet WKY rats (Fig. 4C and E). The compound was shown to exert a preventive role for cardiovascular disease through its active metabolite 5-methyltetrahydrofolate, which can improve the NO bioavailability by increasing NO production as well as by directly scavenging superoxide radicals.<sup>42</sup> The high-salt diet also impeded the accumulation of tetrahydrofolic acid, a precursor of 5-methyltetrahydrofolate, and hampered the production of tetrahydrobiopterin, a regulator of NO synthase known to be a potential therapy for pulmonary hypertension.<sup>43</sup>

Furthermore, SISE intervention in SHR rats led to the upregulation of cardiovascular protective metabolites, including 5-hydroxytryptamine (5-HT), 8,9-epoxyeicosatrienoic acids (8,9-EET), and oleanoic acid (Fig. 4E). Among them, elevated 8,9-EET and oleanoic acid levels improved renal function, and showed antihypertensive effects in angiotensin-II-induced and glucocorticoid-induced hypertension<sup>44</sup> while 5-HT is an important mediator of every major gut-related function. In comparison, the high-salt diet in WKY rats reduced the levels of cardiovascular protective compound L-DOPA, which is converted to dopamine in the kidneys, and plays a role in the regulation of renal function and blood pressure.<sup>45</sup> The high-salt diet in WKY rats also increased the levels of the heart harmful metabolite of 15-hydroxyeicosatetraenoic acid (HETE), while SISE intervention in high-salt diet WKY rats reduced the accumulation of heart harmful metabolite 5-HETE (Fig. 4E). Both 5-HETE and 15-HETE are associated with an increased risk of atherosclerosis and coronary heart disease.<sup>46</sup> On the other hand, the high-salt diet in WKY rats enriched the metabolites related to bile acid biosynthesis and bile secretion, such as cholic acid and taurocholic acid, while SISE intervention

restrained bile acid metabolism in high-salt diet WKY rats by downregulating the accumulation of glycocholic and glycoursoxycholic acids (Fig. 4E). The changes in the composition of the bile acid pool are well known to be involved in the progression of metabolic disorders, diabetes, and obesity.<sup>47</sup> We also performed GC-MS to quantify the levels of short-chain fatty acids (SCFAs) including acetic acid, butyric acid, and propionic acid, which mediate the concentration-dependent dilatation of rat tail arteries,<sup>2</sup> and found that SISE intervention did not substantially affect the SCFAs levels in the faeces of SHR and high-salt diet WKY rats (ESI Fig. S5†).

### 3.5. Correlations between the gut microbiome and metabolome

We next determined whether there are strong associations between the gut microbiome and metabolome. The increased metabolites of dihydrofolic acid in faecal samples were positively correlated with the SISE-enriched bacteria *Roseburia* at a significant level of  $P < 0.01$  (Fig. 5). Previous work indicated that *Roseburia* might be involved in the metabolism of folic acid.<sup>48</sup> Furthermore, *Roseburia* was positively correlated with several beneficial metabolites including 5-HT, oleanoic acid, 8,9-EET, and tetrahydrofolic acid, but negatively correlated with the harmful metabolites 15-HETE and 5-HETE. Of particular interest, 15-HETE was positively correlated with the high-salt diet-increased *Ruminococcus* 1 and the SISE-eliminated *Prevotellaceae* NK3B31 and UCG 001, while negatively correlated with the SISE-enriched *Faecalibaculum* and *Oscillibacter* (Fig. 5).

### 3.6. Distinguishable renal transcriptome

Previous studies have shown that a high-fiber diet could modify the renal transcriptome and improve kidney function by regulating the key pathways and genes involved in cardiovascular health.<sup>8</sup> We, therefore, performed RNA-seq to investigate whether SISE intervention could alter the renal transcriptome in SHR and high-salt diet WKY rats. We found that the renal transcriptomes of these SHR and high-salt diet WKY rats after SISE intervention differed from those fed with the control diet (Fig. 6A and B). Compared with those of rats fed with the control diet, 179 genes were differentially expressed in the kidneys of SHR rats after SISE intervention, 1630 genes were differentially expressed in the kidneys of WKY rats that received the high-salt diet, and 184 genes were differentially expressed in the kidneys of high-salt diet WKY rats after SISE intervention (Fig. 6C). Notably, a total of 147, 1537, and 151 genes were distinguished as differentially expressed in the SISE administrated SHR rats, the high-salt diet WKY rats, and the SISE treated high-salt diet WKY rats (Fig. 6C), respectively.

A high-salt diet might lead to the upregulation of the renin-angiotensin system and calcium signaling in high-salt diet WKY rats through the upregulation of the gene encoding for the angiotensin I converting enzyme (Ace), the alpha-2/delta subunit (*Cacnα2δ2*) (Fig. 6E, ESI Fig. S6A†), a putative calcium channel accessory subunit in L-type voltage-dependent calcium channel (LTCC), and is associated with impaired

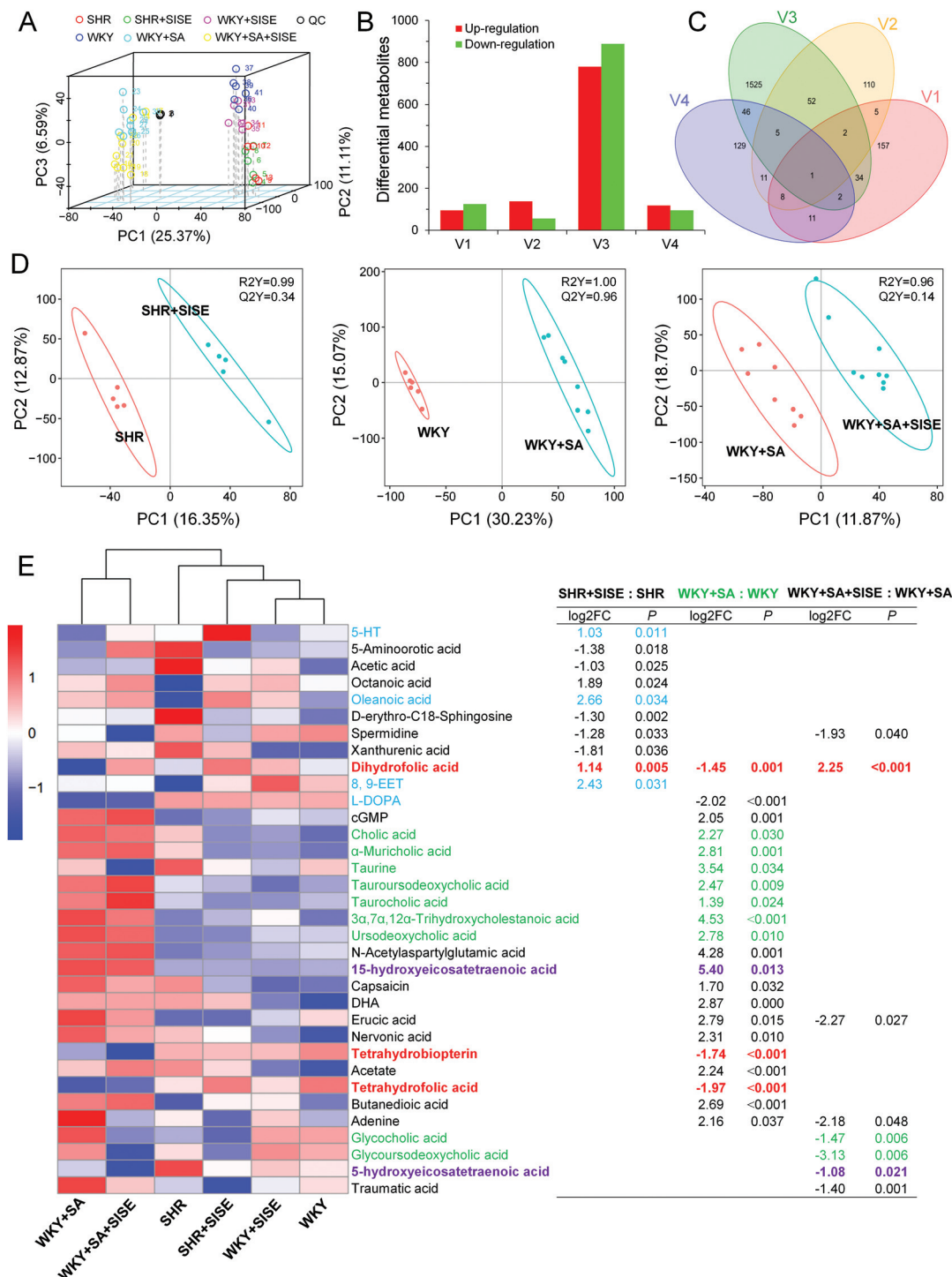


**Fig. 4** SISE intervention alters the gut microbiota metabolome of SHR and high-salt diet WKY rats. Principal component analysis based on faecal metabolites (A). The differential metabolites (B) and Venn diagram (C) in different comparisons, showing differential metabolites in common between SHR and high-salt diet WKY rats after receiving SISE intervention. (D) The PLS-DA score plots based on faecal metabolites for each comparison. (E) A heatmap of differential metabolites potentially associated with cardiovascular disease in each treatment. The scale reflects the data, where red indicates high values, whereas blue indicates low values for the quantitative levels of differential metabolites that were classified at that rank. log2FC, log 2 fold-change; QC, quality control; 5-HT, 5-hydroxytryptamine; 8,9-EET, 8,9-epoxyeicosatrienoic acids; DHA, docosahexaenoic acid; V1, V2, V3, and V4 represent comparisons of the gut metabolome between SHR + SISE and SHR, between WKY + SISE and WKY, between WKY + SA and WKY, and between WKY + SA + SISE and WKY + SA, respectively.

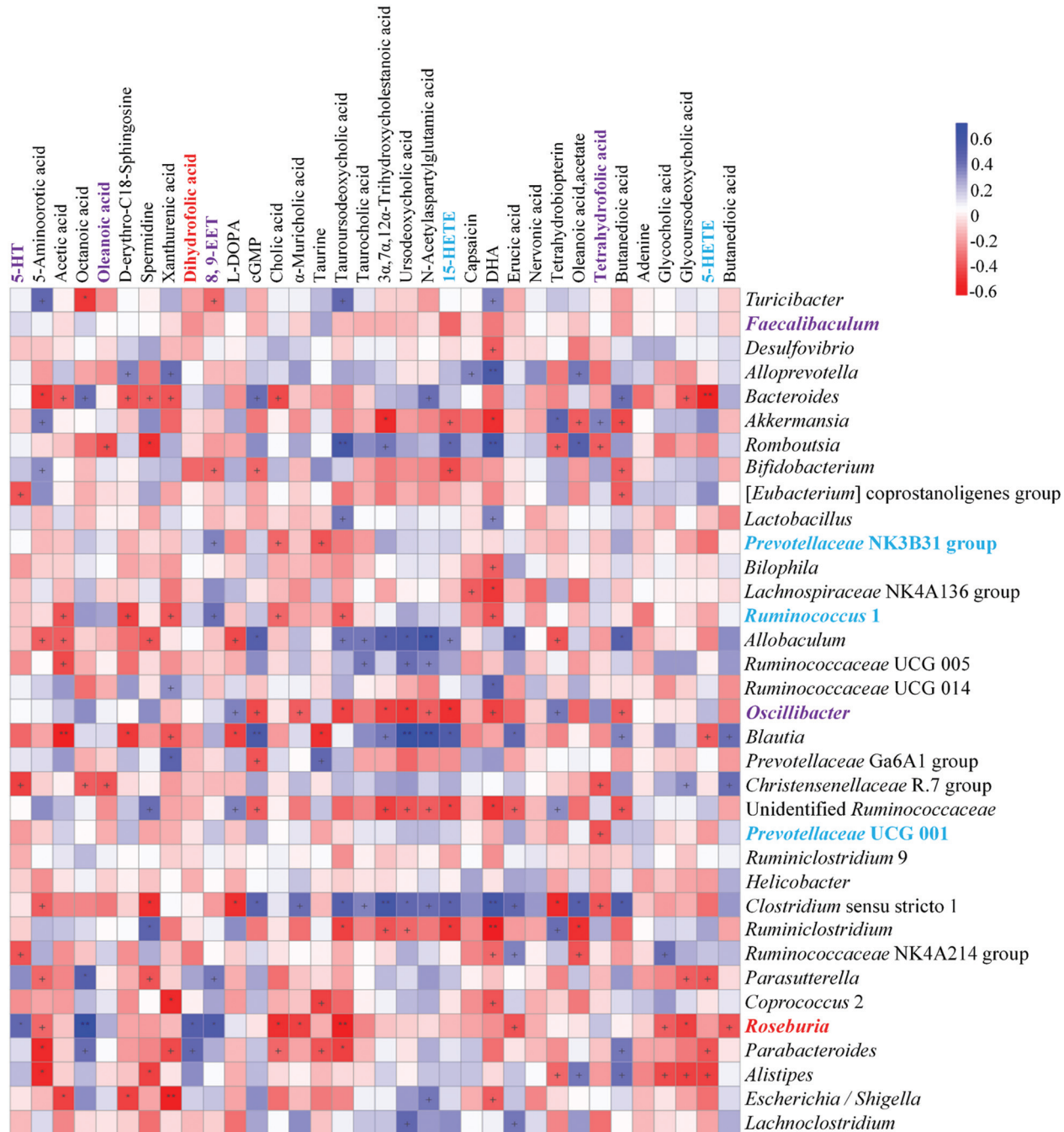


**Fig. 5** Correlation analysis of the microbiome and metabolome. Spearman's correlation coefficients between the abundance of the top 35 genera and the level of faecal metabolic patterns were calculated. The scale reflects the data as follows: blue indicates a positive correlation, whereas red indicates a negative correlation between gut bacteria and metabolites. +,  $P < 0.05$ ; \* $P < 0.01$ ; \*\* $P < 0.001$ .

$\text{Ca}^{2+}$  homeostasis, left ventricular hypertrophy and heart failure,<sup>49</sup> and subunit alpha1 S (*Cacna1s*) (Fig. 6E, ESI Fig. S6B†), a voltage sensor that generates signals in LTCC.<sup>50</sup> On the contrary, SISE intervention in high-salt diet WKY rats could lower calcium signaling through downregulation of the gene expressions of *Cacna2d2* and *Cacna1s*. SISE intervention in high-salt diet WKY rats also reduced the Wnt-mediated

blood pressure regulation signaling (Fig. 6E).<sup>51</sup> SISE intervention in SHR rats also lowered calcium signaling by downregulation of the gene for calcium/calmodulin-dependent protein kinase II gamma (*Camk2g*) (Fig. 6E, ESI Fig. S6C†), a ubiquitous mediator and activator of LTCC,<sup>52</sup> whose expression level was elevated in SHR rats as compared with that in WKY rats (Fig. 6E). It is interesting to note that SISE intervention pre-

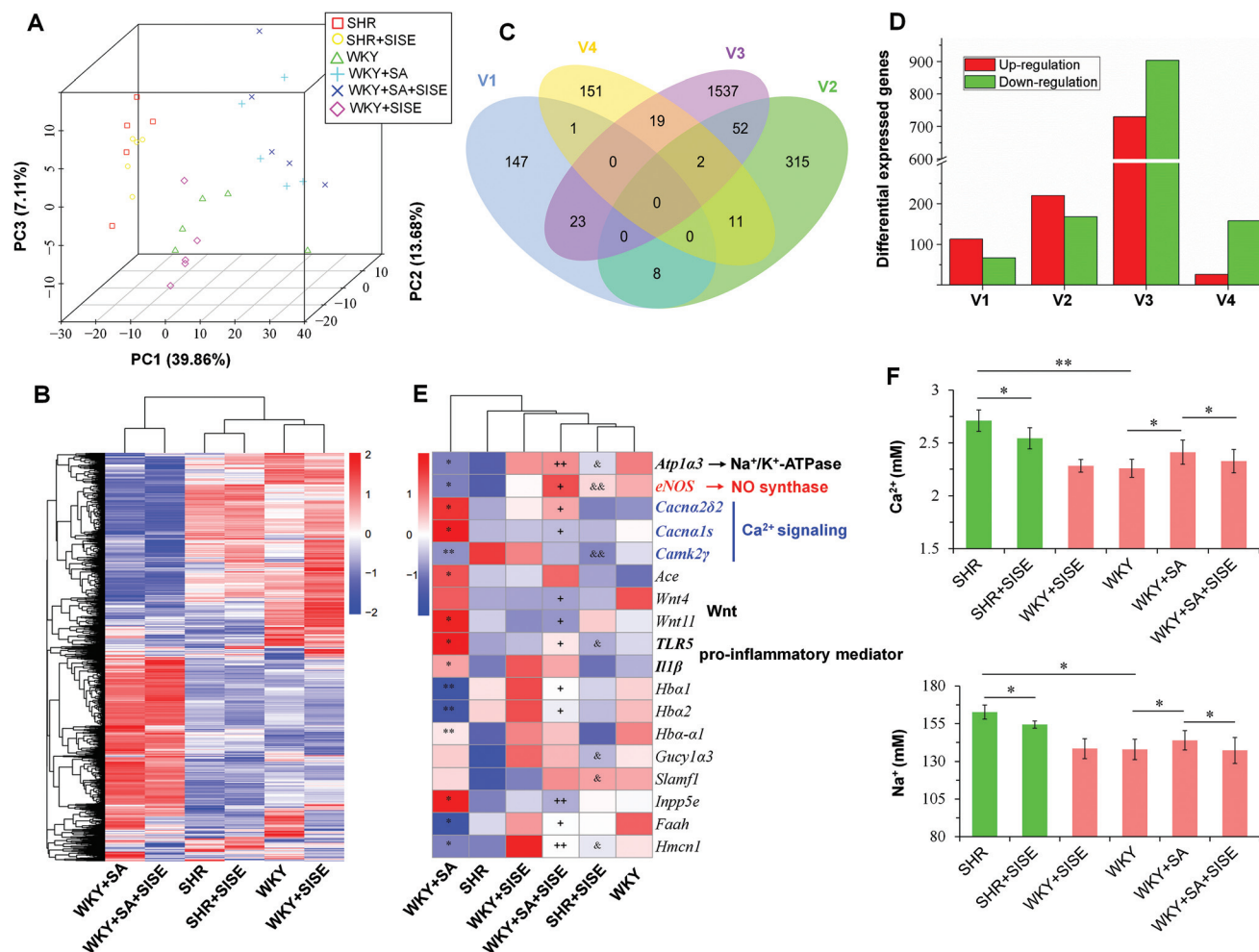


**Fig. 6** SISE intervention modifies the renal transcriptome of SHR and high-salt diets in WKY rats. Principal component analysis (A) and hierarchical clustering (B) of the renal transcriptome showing that SHR rats and high-salt diet WKY rats, after SISE intervention, formed a distinctive group from those fed the control diet. Venn diagram of the renal transcriptome (C), showing differentially expressed genes in common between SHR and high-salt diet WKY rats after receiving SISE intervention. The differentially expressed genes in different comparisons (D). V1, V2, V3, and V4 represent comparisons of the renal transcriptome between SHR + SISE and SHR, between WKY + SISE and WKY, between WKY + SA and WKY, and between WKY + SA + SISE and WKY + SA, respectively. (E) A heatmap of differentially expressed genes potentially associated with cardiovascular disease in each group. The scale reflects the data as follows: red indicates high values, whereas blue indicates low values for the percentages of differentially expressed genes that were classified at that rank. \*  $P < 0.05$ , \*\*  $P < 0.01$ , the WKY + SA group compared with the WKY group; <sup>a</sup>  $P < 0.05$ , <sup>aa</sup>  $P < 0.01$ , the WKY + SA + SISE group compared with the WKY + SA group; <sup>b</sup>  $P < 0.05$ , <sup>bb</sup>  $P < 0.01$ , the SHR + SISE group compared with the SHR group. SISE intervention ameliorates plasma  $\text{Ca}^{2+}$  and  $\text{Na}^+$  (F) levels in SHR and high-salt diet WKY rats; \*,  $P < 0.05$ ; \*\*,  $P < 0.01$ .

vented the decrease in the gene expression levels of *Atp1a3* coding for the  $\text{Na}^+/\text{K}^+$ -ATPase subunit and *eNOS* coding for NO synthase in SHR and high-salt diet WKY rats (Fig. 6E).

Similarly, we also observed the upregulation of the pro-inflammatory mediators interleukin-1 (*IL-1*) signaling system through the elevated expression of the gene encoding for toll-like receptor 5 (TLR5), and downregulation of the genes believed to have a preventive role in hypertension, such as the gene for  $\alpha 1$  hemoglobin (Hba-a2) in high-salt diet WKY rats (Fig. 6E), which is involved in the negative regulation of blood pressure.<sup>53</sup> Significantly, SISE intervention in high-salt diet WKY rats reversed the expression levels of these genes (Fig. 6E) and normalized the expression of these genes to levels comparable to those of WKY rats. SISE intervention in SHR rats might

promote the magnitude of immune response by upregulation of the gene for signaling lymphocytic activation molecule family member 1 (Slamf1) (Fig. 6E), which is associated with B cell proliferation and immunoglobulin synthesis.<sup>54</sup> SISE also upregulated the gene for a subunit of soluble guanylate cyclase (Gucy1a3) (Fig. 6E), which plays a role in vasodilation by the mediation of cGMP synthesis.<sup>53</sup> Notably, SHR rats showed blunted expression of the *Slamf1* and *Gucy1a3* genes as compared with WKY rats (Fig. 6E).

### 3.7. SISE intervention ameliorates plasma $\text{Ca}^{2+}$ and $\text{Na}^+$ homeostasis

Changes in salt intake content can modify  $\text{Ca}^{2+}$  handling, and alterations in myocardial  $\text{Ca}^{2+}$  handling have been noticed at

the early stages prior to the development of heart failure.<sup>55</sup> We found higher plasma Ca<sup>2+</sup> levels in SHR and high-salt diet WKY rats as compared with WKY rats (Fig. 6F), while SISE intervention attenuated the plasma Ca<sup>2+</sup> levels in SHR rats, and significantly reversed them to normal levels in high-salt diet WKY rats (Fig. 6F). These findings indicate that SISE intervention could ameliorate plasma Ca<sup>2+</sup> homeostasis in SHR and high-salt diet WKY rats. Similarly, SISE intervention also prevented the expansion of serum Na<sup>+</sup> levels in SHR and high-salt diet WKY rats (Fig. 6F).

### 3.8. Correlations among oxidative damage, gut metabolome, and renal transcriptome

We also performed correlation analysis to evaluate the associations between oxidative damage, gut metabolome, as well as gut metabolome and renal transcriptome. As shown in Fig. 7, the gut increased metabolite of dihydrofolic acid was negatively correlated with the gene expression levels of renal calcium signaling of *Cacna2d2* and *Cacna1s*. Moreover, dihydrofolic acid was positively correlated with the oxidative damage characteristics of SOD and GSH, but negatively correlated with the oxidative damage level of MDA. The tetrahydro-

folic acid was also negatively correlated with the gene expression levels of the renal calcium signaling of *Cacna2d2*, but positively correlated with the gene expression levels of *eNOS* and the oxidative damage characteristics of NO and GSH (Fig. 7).

## 4. Discussion

Previous studies have indicated that aberrant gut microbiota contribute to the pathogenesis of hypertension.<sup>3,5,14</sup> In this study, by using SHR rats and WKY rats as animal models for the high-salt diet, we showed that SISE intervention attenuated oxidative damage, restored plasma Ca<sup>2+</sup> homeostasis, lowered cardiac hypertrophy and lowered blood pressure. We also demonstrated that SISE intervention changed the gut microbiome and metabolome and, in particular, increased the prevalence of *Roseburia*, and improved the levels of gut-derived dihydrofolic acid. Furthermore, we found that SISE intervention could modulate the renal molecular pathways beneficial for cardiovascular function, particularly the L-type voltage-dependent calcium channel. These findings showed for the

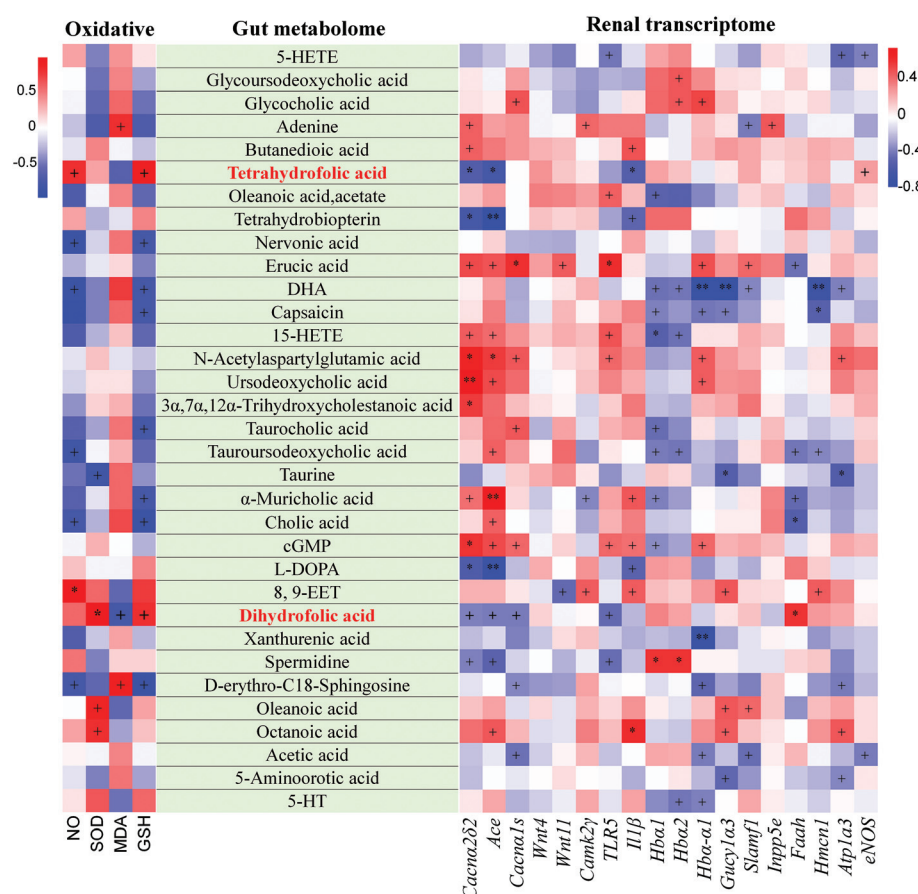


**Fig. 7** Correlation analysis among oxidative damage, gut metabolome, and renal transcriptome. Spearman's correlation coefficients between the characteristics of oxidative damage and the levels of faecal metabolic patterns, as well as the levels of faecal metabolic patterns and expression levels of differentially expressed genes, were calculated. The scale reflects the data as follows: blue indicates positive correlations, whereas red indicates negative correlations. +,  $P < 0.05$ ; \* $P < 0.01$ ; \*\*,  $P < 0.001$ .

first time that plant phytochemicals can effectively alleviate hypertension by altering the gut microbiota and metabolome.

Our data have shown that in general, SISE intervention exerts dual effects on gut microbiota, *i.e.*, increases the prevalence of bacteria negatively related to hypertension, but reduces the levels of the bacteria positively associated with hypertension. The gut microbiota of hypertensive humans and animals are associated with decreased levels of beneficial bacteria, such as *Roseburia*, *Faecalibacterium* and *Lactobacillus*, and the prevalence of harmful bacteria, such as *Prevotella*.<sup>5,14</sup> Several intestinal bacteria are affected by high-salt diets, and are, therefore, associated with the increased frequency of hypertension.<sup>56</sup> Consistent with the previous reports,<sup>3</sup> a high-salt diet in WKY rats increased the F/B ratio and suppressed the beneficial *Roseburia* and *Lactobacillus*, while SISE intervention reversed and normalized the F/B ratio, as well as restored the levels of *Roseburia* and *Lactobacillus*. We also found that SISE intervention in SHR rats significantly increased the F/B ratio, as well as enhanced the bacterial levels that are negatively correlated with hypertension, including *Roseburia* and *Faecalibacterium*. Probiotic *Lactobacillus* exerts cardiovascular-protective effects in genetic hypertension,<sup>7</sup> while *Roseburia* and *Faecalibacterium* are also distributed abundantly in the healthy control microbiomes of many chronic diseases, including hypertension,<sup>40</sup> type 2 diabetes,<sup>57</sup> and liver cirrhosis.<sup>58</sup> These bacteria are usually associated with intestinal microbial homeostasis and production of SCFAs,<sup>59,60</sup> and may protect against hypertension.<sup>61</sup> In addition, we observed that SISE intervention further reduced the prevalence of harmful bacteria in SHR and high-salt diet WKY rats, including those frequently distributed in the hypertensive gut microbiome of *Bacteroides*, *Alloprevotella*, *Prevotella*, and *Ruminococcus*. Although fiber has been shown to increase the prevalence of *Bacteroides acidifaciens* in mineralocorticoid-excess induced hypertensive mice,<sup>8</sup> several *Bacteroides* species were also enriched in the hypertensive gut microbiome,<sup>40</sup> which are considered as generally opportunistic pathogens in gastrointestinal infections.<sup>62</sup> *Alloprevotella* and *Prevotella* may play important roles in the pathology of hypertension by triggering epithelial inflammatory responses.<sup>5,63</sup> Overall, our observations suggest that SISE may alleviate hypertension by altering the F/B ratio, as well as by changing the levels of other specific bacteria.

The gut microbiota may play an active role in the development of complex metabolic abnormalities associated with various diseases, such as susceptibility to insulin resistance, non-alcoholic fatty liver disease, and cardiovascular disease.<sup>2</sup> Previous work has indicated that a gut-flora-generated metabolite of dietary choline and phosphatidylcholine, *i.e.*, trimethylamine N-oxide (TMAO), could promote the development of atherosclerosis.<sup>64</sup> High-salt intake depletes *Lactobacillus murinus* and may induce salt-sensitive hypertension by substantially influencing the levels of faecal tryptophan metabolites.<sup>3,4</sup> A high-fiber diet was shown to ameliorate heart function in the experimental hypertension model by increasing the production of SCFAs, such as acetate, with the elevated levels of *Bacteroides acidifaciens*.<sup>65</sup> Here, we have shown that

SISE intervention in high-salt diet WKY rats reduced the cardiovascular harmful metabolites, including 5-HETE, while the high-salt diet in WKY rats enriched the heart-harmful metabolite 15-HETE, which are the well-characterized products of 5- and 15-lipoxygenases (5-, 15-LO) activity, respectively. 5-LO activity is essential for leukotriene biosynthesis and is, therefore, linked to several inflammatory pathologies, while 15-LO/15-HETE signaling plays a role in platelet activation and pulmonary vascular thrombosis in pulmonary hypertension.<sup>66</sup> We also observed that SISE intervention in SHR and high-salt diet WKY rats enriched the cardiovascular protective metabolites including dihydrofolic acid, and in contrast, a high-salt diet in WKY rats reduced the cardiovascular protective metabolites dihydrofolic acid, tetrahydrofolic acid, and tetrahydrobiopterin. Dihydrofolic and tetrahydrofolic acids are the precursors of 5-methyl tetrahydrofolate, which plays a key role in circulating levels of NO, and may promote vascular protection by improving the redox status through increasing NO bioavailability and decreasing superoxide ( $O_2^-$ ) production.<sup>67</sup> These findings support the notion that the metabolite of dihydrofolic acid could be a potential therapeutic component for preventing the progression of hypertension. Consistent with this notion, we discovered a significant positive correlation between high dihydrofolic acid levels and SISE-enriched bacteria such as *Roseburia*. Overall, these observations suggest that SISE may produce antihypertensive effects by altering the gut microbiota metabolome *via* increasing the cardiovascular protective metabolites, in particular, dihydrofolic acid, and decreasing the cardiovascular harmful metabolites.

The kidneys play a central role in regulating blood pressure. A recent investigation elucidated that SHR rats exhibited alterations in left atrial  $Ca^{2+}$  handling early after the development of hypertension, which may serve as a trigger for atrial tachyarrhythmias.<sup>68</sup> Furthermore, previous reports have suggested that altered calcium homeostasis, as exhibited by increased calcium excretion, is associated with elevated blood pressure levels.<sup>69</sup> In this work, the plasma  $Ca^{2+}$  dyshomeostasis found in SHR and high-salt diet WKY rats was ameliorated after SISE intervention. The complex machinery, including LTCC, maintains that the  $Ca^{2+}$  homeostasis, and hypertensive individuals may have altered renal handling of calcium.<sup>70</sup> Our renal transcriptome data support that high-salt diets upregulate calcium signaling with increased expression of the *Cacna2d2* subunit and *Cacna1s* voltage sensor of LTCC in WKY rats, thereby indicating the exacerbated  $Ca^{2+}$  influx through LTCC. In this regard, it is interesting to note that SISE intervention could reduce calcium signaling with a lowered expression of the *Cacna1s* subunit, *Cacna1s* voltage sensor, and co-regulator *Camk2γ* of LTCC in high-salt diet WKY and SHR rats, respectively. Many studies have indicated that NaCl retention and a tendency toward plasma volume expansion is involved in the chronic elevation of blood pressure.<sup>71</sup> The  $Na^+/K^+$ -ATPase pump in the cell membrane transports  $Na^+$  into the cell and establishes the maintenance of an electrochemical gradient for  $Na^+$  across the cell membrane directed inwards. In the present study, SISE intervention prevented the expansion of

serum Na<sup>+</sup> levels and inhibited the decrease in the expression level of *Atp1a3* coding for the Na<sup>+</sup>/K<sup>+</sup>-ATPase subunit in SHR and high-salt diet WKY rats. These results were in line with previous reports that the tartary buckwheat and common buckwheat treatment prevented the increase of serum Na<sup>+</sup> and decrease of Na<sup>+</sup>/K<sup>+</sup>-ATPase expression levels.<sup>39</sup> Cumulatively, these findings suggest that the antihypertensive effect of SISE might also be related to its activity in remodeling Ca<sup>2+</sup> and Na<sup>+</sup> homeostasis by the regulation of LTCC and Na<sup>+</sup>/K<sup>+</sup>-ATPase, respectively.

The oxidative stress was involved in the initiation and progression of hypertension in animal models.<sup>72</sup> ROS, such as O<sub>2</sub><sup>•-</sup>, were shown to stimulate Ca<sup>2+</sup> entry through LTCC in vascular smooth muscle cells and in cardiomyocytes,<sup>73</sup> while NO production can exert rapid modulatory effects on Ca<sup>2+</sup> homeostasis. The imbalance between O<sub>2</sub><sup>•-</sup> and NO production in the kidneys is a primary determinant in renal oxidative stress, leading to salt-sensitive hypertension.<sup>74</sup> The renal transcriptome data found that SISE intervention prevented the decrease in the gene expression level of *eNOS* coding for NO synthase in SHR and high-salt diet WKY rats. Moreover, NO generation is correlated with blood pressure regulation in angiotensin II-induced hypertension.<sup>75</sup> Concomitantly, 5-methyltetrahydrofolate, the circulating active form of dihydrofolic acid and tetrahydrofolic acid, improves NO production while reducing superoxide production.<sup>67</sup> In this study, the correlation analysis supported that dihydrofolic acid was negatively correlated with the gene expression levels of the renal calcium signaling of *Cacna2d2* and *Cacna1s* and oxidative damage levels of MDA, but was positively correlated with the oxidative damage characteristics of SOD and GSH. The tetrahydrofolic acid was also negatively correlated with the gene expression levels of *Cacna2d2*, but positively correlated with the gene expression levels of *eNOS* and the levels of NO and GSH. These findings suggest the potential that SISE might act to influence hypertension, as the results in this study showed that SISE intervention substantially attenuated oxidative damage, enriched gut dihydrofolic acid, and remodeled Ca<sup>2+</sup> and Na<sup>+</sup> homeostasis by the regulation of LTCC and Na<sup>+</sup>/K<sup>+</sup>-ATPase in SHR and high-salt diet WKY rats. Consistent with this hypothesis, a recent work reported that a buckwheat-enriched diet ameliorated high salt-induced hypertension by scavenging O<sub>2</sub><sup>•-</sup> and by preventing the high salt-induced decreases in NO bioavailability through the Na<sup>+</sup>/K<sup>+</sup>-ATPase pump in kidneys.<sup>39</sup>

It is interesting to note that polysaccharides isolated from different materials can reduce obesity, inflammation, and insulin resistance in mice fed a high-fat diet by decreasing gut dysbiosis.<sup>76,77</sup> In addition, the polyphenols could prevent high-fat/high-sucrose diet-induced obesity, and may exert cardiovascular health benefits.<sup>78-80</sup> The Sacha inchi (*Plukenetia volubilis* L.) shell is regarded as a novel and alternative source of phenolic compounds and antioxidants,<sup>12</sup> but the biological functions of its components in protection of living organisms have not yet been characterized. The next challenge would be to identify and characterize the key component(s) of SISE contributing to its biological effects on hypertension.

In summary, the results from this study unveiled for the first time that SISE intervention could significantly attenuate the development of hypertension and cardiac hypertrophy in SHR and high-salt diet WKY rats. The antihypertension effect of SISE is related to its potent activities in modulating the gut microbiome and metabolome, in particular, through increasing the genus *Roseburia* and metabolite dihydrofolic acid, remodeling of Ca<sup>2+</sup> homeostasis through LTCC with the redox modulation, and alleviating cardiac hypertrophy. Our data present further evidence for the critical role of gut microbiota in the pathogenesis of hypertension, and extend the mechanism of the gut–kidney–heart axis,<sup>8</sup> and importantly, provide mechanistic insights into the protective actions of SISE on hypertension, which might provide useful clues for developing new dietary strategies for the prevention of hypertension.

## Conflicts of interest

The authors declare no conflicts of interest.

## Acknowledgements

We thank Novogene (Beijing, China) for the use of Illumina platform. We also thank Prof Shaoyong Chen (Hematology-Oncology Division, Beth Israel Deaconess Medical Center, Harvard Medical School) for the helpful advice and guidance with the analysis of gut metabolome data presented in this study. This work was supported by Natural Science Foundation of Guangdong Province (2020A151501268) and Key-Area Research and Development Program of Guangdong Province (2020B020226008).

## References

- 1 D. Mozaffarian, E. J. Benjamin, A. S. Go, D. K. Arnett, M. J. Blaha, M. Cushman, S. R. Das, S. de Ferranti, J.-P. Després, H. J. Fullerton, V. J. Howard, M. D. Huffman, C. R. Isasi, M. C. Jiménez, S. E. Judd, B. M. Kissela, J. H. Lichtman, L. D. Lisabeth, S. Liu, R. H. Mackey, D. J. Magid, D. K. McGuire, E. R. Mohler, C. S. Moy, P. Muntner, M. E. Mussolini, K. Nasir, R. W. Neumar, G. Nichol, L. Palaniappan, D. K. Pandey, M. J. Reeves, C. J. Rodriguez, W. Rosamond, P. D. Sorlie, J. Stein, A. Towfighi, T. N. Turan, S. S. Virani, D. Woo, R. W. Yeh and M. B. Turner, Heart disease and stroke statistics—2016 update: A report from the american heart association, *Circulation*, 2016, **133**, e38–e48.
- 2 F. Z. Marques, C. R. Mackay and D. M. Kaye, Beyond gut feelings: how the gut microbiota regulates blood pressure, *Nat. Rev. Cardiol.*, 2018, **15**, 20–32.
- 3 N. Wilck, M. G. Matus, S. M. Kearney, S. W. Olesen, K. Forslund, H. Bartolomaeus, S. Haase, A. Mähler, A. Balogh and L. Markó, Salt-responsive gut commensal

- modulates TH17 axis and disease, *Nature*, 2017, **551**, 585–589.
- 4 Z. Zhang, J. Zhao, C. Tian, X. Chen, H. Li, X. Wei, W. Lin, N. Zheng, A. Jiang, R. Feng, J. Yuan and X. Zhao, Targeting the gut microbiota to investigate the mechanism of lactulose in negating the effects of a high-salt diet on hypertension, *Mol. Nutr. Food Res.*, 2019, **63**, 1800941.
  - 5 J. Li, F. Zhao, Y. Wang, J. Chen, J. Tao, G. Tian, S. Wu, W. Liu, Q. Cui and B. Geng, Gut microbiota dysbiosis contributes to the development of hypertension, *Microbiome*, 2017, **5**, 14.
  - 6 M. M. Santisteban, S. Kim, C. J. Pepine and M. K. Raizada, Brain–Gut–Bone Marrow Axis: Implications for hypertension and related therapeutics, *Circ. Res.*, 2016, **118**, 1327–1336.
  - 7 M. Gómez-Guzmán, M. Toral, M. Romero, R. Jiménez, P. Galindo, M. Sánchez, M. J. Zarzuelo, M. Olivares, J. Gálvez and J. Duarte, Antihypertensive effects of probiotics *Lactobacillus* strains in spontaneously hypertensive rats, *Mol. Nutr. Food Res.*, 2016, **59**, 2326–2336.
  - 8 F. Z. Marques, E. Nelson, P. Y. Chu, D. Horlock, A. Fiedler, M. Ziemann, J. K. Tan, S. Kuruppu, N. W. Rajapakse and A. Elosta, High-fiber diet and acetate supplementation change the gut microbiota and prevent the development of hypertension and heart failure in hypertensive mice, *Circulation*, 2017, **135**, 964–977.
  - 9 P. V. Bauer, F. A. Duca, T. Waise, B. A. Rasmussen, M. A. Abraham, H. J. Dranse, A. Puri, C. A. O'Brien and T. Lam, Metformin alters upper small intestinal microbiota that impact a glucose-SGLT1-sensing glucoregulatory pathway, *Cell Metab.*, 2018, **27**, 101–117.
  - 10 H. H. Yoo, I. S. Kim, D. H. Yoo and D. H. Kim, Effects of orally administered antibiotics on the bioavailability of amlodipine: gut microbiota-mediated drug interaction, *J. Hypertens.*, 2016, **34**, 156–162.
  - 11 P. Li, J. Wen, X. Ma, F. Lin, Z. Jiang and B. Du, Structural, functional properties and immunomodulatory activity of isolated Inca peanut (*Plukenetia volubilis*, L.) seed albumin fraction, *Int. J. Biol. Macromol.*, 2018, **118**, 1931–1941.
  - 12 S. Wang, F. Zhu and Y. Kakuda, Sacha inchi (*Plukenetia volubilis* L.): Nutritional composition, biological activity, and uses, *Food Chem.*, 2018, **265**, 316–328.
  - 13 X. Cai, X.-W. Ma, P. Li, Y. Yang and B. Du, Study on anti-hypertensive effect of Sacha inchi shell water extract, *Food Res. Dev.*, 2019, **40**, 87–92.
  - 14 T. Yang, M. M. Santisteban, V. Rodriguez, E. Li, N. Ahmari, J. M. Carvajal, M. Zadeh, M. Gong, Y. Qi and J. Zubcevic, Gut dysbiosis is linked to hypertension, *Hypertension*, 2015, **65**, 1331–1340.
  - 15 M. M. Santisteban, Y. Qi, J. Zubcevic, S. Kim, T. Yang, V. Shenoy, C. T. Cole-Jeffrey, G. O. Lobaton, D. C. Stewart, A. Rubiano, C. S. Simmons, F. Garcia-Pereira, R. D. Johnson, C. J. Pepine and M. K. Raizada, Hypertension-linked pathophysiological alterations in the gut, *Circ. Res.*, 2017, **120**, 312–323.
  - 16 J. Zubcevic, E. M. Richards, T. Yang, S. Kim, C. Sumners, C. J. Pepine and M. K. Raizada, Impaired autonomic nervous system-microbiome circuit in hypertension, *Circ. Res.*, 2019, **125**, 104–116.
  - 17 S. Chakraborty, S. Galla, X. Cheng, J.-Y. Yeo, B. Mell, V. Singh, B. Yeoh, P. Saha, A. V. Mathew, M. Vijay-Kumar and B. Joe, Salt-responsive metabolite, β-hydroxybutyrate, attenuates hypertension, *Cell Rep.*, 2018, **25**, 677–689.
  - 18 Y. Li, D. Chen, C. Xu, Q. Zhao, Y. Ma, S. Zhao and C. Chen, Glycolipid metabolism and liver transcriptomic analysis of the therapeutic effects of pressed degreased walnut meal extracts on type 2 diabetes mellitus rats, *Food Funct.*, 2020, **11**, 5538–5552.
  - 19 Y. Li, Y. Chu, L. Yu, H. Kang and L. Zhou, Transcriptomic analysis of Bama pig's liver in various nutritional states reveals a metabolic difference of fatty acids, *Food Funct.*, 2017, **8**, 3480–3490.
  - 20 R. Del Pino-García, M. D. Rivero-Pérez, M. L. González-SanJosé, K. D. Croft and P. Muñiz, Antihypertensive and antioxidant effects of supplementation with red wine pomace in spontaneously hypertensive rats, *Food Funct.*, 2017, **8**, 2444–2454.
  - 21 P. Li, J. Deng, N. Xiao, X. Cai, Q. Wu, Z. Lu, Y. Yang and B. Du, Identification of polyunsaturated triacylglycerols and C=C location isomers in sacha inchi oil by photochemical reaction mass spectrometry combined with nuclear magnetic resonance spectroscopy, *Food Chem.*, 2020, **307**, 125568.
  - 22 A. Howe, D. L. Ringus, R. J. Williams, Z.-N. Choo, S. M. Greenwald, S. M. Owens, M. L. Coleman, F. Meyer and E. B. Chang, Divergent responses of viral and bacterial communities in the gut microbiome to dietary disturbances in mice, *ISME J.*, 2015, **10**, 1217.
  - 23 R. C. Edgar, UPARSE: highly accurate OTU sequences from microbial amplicon reads, *Nat. Methods*, 2013, **10**, 996–998.
  - 24 J. G. Caporaso, J. Kuczynski, J. Stombaugh, K. Bittinger, F. D. Bushman, E. K. Costello, N. Fierer, A. G. Pena, J. K. Goodrich and J. I. Gordon, QIIME allows analysis of high-throughput community sequencing data, *Nat. Methods*, 2010, **7**, 335–336.
  - 25 X. C. Morgan, T. L. Tickle, H. Sokol, D. Gevers, K. L. Devaney, D. V. Ward, J. A. Reyes, S. A. Shah, N. Leleiko and S. B. Snapper, Dysfunction of the intestinal microbiome in inflammatory bowel disease and treatment, *Genome Biol.*, 2012, **13**, R79.
  - 26 P. Zhou, H. Fan, T. Lan, X.-L. Yang, W.-F. Shi, W. Zhang, Y. Zhu, Y.-W. Zhang, Q.-M. Xie, S. Mani, X.-S. Zheng, B. Li, J.-M. Li, H. Guo, G.-Q. Pei, X.-P. An, J.-W. Chen, L. Zhou, K.-J. Mai, Z.-X. Wu, D. Li, D. E. Anderson, L.-B. Zhang, S.-Y. Li, Z.-Q. Mi, T.-T. He, F. Cong, P.-J. Guo, R. Huang, Y. Luo, X.-L. Liu, J. Chen, Y. Huang, Q. Sun, X.-L.-L. Zhang, Y.-Y. Wang, S.-Z. Xing, Y.-S. Chen, Y. Sun, J. Li, P. Daszak, L.-F. Wang, Z.-L. Shi, Y.-G. Tong and J.-Y. Ma, Fatal swine acute diarrhoea syndrome caused by an HKU2-related coronavirus of bat origin, *Nature*, 2018, **556**, 255–258.
  - 27 D. Kim, B. Langmead and S. L. Salzberg, HISAT: a fast spliced aligner with low memory requirements, *Nat. Methods*, 2015, **12**, 357–360.

- 28 M. D. Young, M. J. Wakefield, G. K. Smyth and A. Oshlack, Gene ontology analysis for RNA-seq: accounting for selection bias, *Genome Biol.*, 2010, **11**, R14.
- 29 X. Mao, T. Cai, J. G. Olyarchuk and L. Wei, Automated genome annotation and pathway identification using the KEGG Orthology (KO) as a controlled vocabulary, *Bioinformatics*, 2005, **21**, 3787–3793.
- 30 S. Adnan, J. W. Nelson, N. J. Ajami, V. R. Venna, J. F. Petrosino, R. M. B. Jr and D. J. Durgan, Alterations in the gut microbiota can elicit hypertension in rats, *Physiol. Genomics*, 2017, **49**, 96–104.
- 31 K. Kumakura, R. Kato, T. Kobayashi, N. Kimura, H. Takahashi, A. Takahashi and H. Matsuoka, The salted radish takuan-zuke shows antihypertension effects in spontaneously hypertensive rats, *Food Funct.*, 2017, **8**, 3491–3500.
- 32 B. Mell, V. R. Jala, A. V. Mathew, J. Byun, H. Waghulde, Y. Zhang, B. Haribabu, M. Vijay-Kumar, S. Pennathur and B. Joe, Evidence for a link between gut microbiota and hypertension in the Dahl rat, *Physiol. Genomics*, 2015, **47**, 187–197.
- 33 L. da Silva Lara, M. McCormack, H. Kobori, S. Shenouda, D. S. Majid, L. G. Navar and M. C. Prieto, High salt intake exacerbates renal tissue oxidative stress and urinary angiotensinogen excretion during AngII-dependent hypertension, *FASEB J.*, 2010, **24**, 1059.
- 34 Q. Ge, Z. Wang, Y. Wu, Q. Huo, Z. Qian, Z. Tian, W. Ren, X. Zhang and J. Han, High salt diet impairs memory-related synaptic plasticity via increased oxidative stress and suppressed synaptic protein expression, *Mol. Nutr. Food Res.*, 2017, **61**, 1700134.
- 35 C. Wang, Z. Huang, K. Yu, R. Ding, K. Ye, C. Dai and X. Xu, Guanghong Zhou and C. Li, High-salt diet has a certain impact on protein digestion and gut microbiota: a sequencing and proteome combined study, *Front. Microbiol.*, 2017, 01838.
- 36 B. M. Aloud, P. Raj, J. McCallum, C. Kirby, X. L. Louis, F. Jahan, L. Yu, B. Hiebert, T. A. Duhamel, J. T. Wigle, H. Blewett and T. Netticadan, Cyanidin 3-O-glucoside prevents the development of maladaptive cardiac hypertrophy and diastolic heart dysfunction in 20-week-old spontaneously hypertensive rats, *Food Funct.*, 2018, **9**, 3466–3480.
- 37 A. Grabner, A. P. Amaral, K. Schramm, S. Singh, A. Sloan, C. Yanucil, J. Li, L. A. Shehadeh, J. M. Hare and V. David, Activation of cardiac fibroblast growth factor receptor 4 causes left ventricular hypertrophy, *Cell Metab.*, 2015, **22**, 1020–1032.
- 38 A. Gudjoncik, C. Guenancia, M. Zeller, Y. Cottin, C. Vergely and L. Rochette, Iron, oxidative stress, and redox signaling in the cardiovascular system, *Mol. Nutr. Food Res.*, 2014, **58**, 1721–1738.
- 39 D. Cheng, X. Zhang, M. Meng, L. Han, Z. Li, L. Hou, W. Qi and C. Wang, The protective effect of buckwheat-enriched diet on renal injury in high salt-induced hypertension in rat, *Food Funct.*, 2016, **7**, 3548–3554.
- 40 Q. Yan, Y. Gu, X. Li, W. Yang, L. Jia, C. Chen, X. Han, Y. Huang, L. Zhao, P. Li, Z. Fang, J. Zhou, X. Guan, Y. Ding, S. Wang, M. Khan, Y. Xin, S. Li and Y. Ma, Alterations of the gut microbiome in hypertension, *Front. Cell. Infect. Microbiol.*, 2017, **7**, 381.
- 41 R. T. Demmer, P. N. Trinh, A. M. Zuver, D. Onat, N. Akter, E. A. Royzman, J. K. Nwokocha, A. Clemons, F. Castagna, A. Pinsino, A. R. Garan, V. K. Topkara, D. L. Brunjes, K. Takeda, H. Takayama, Y. Naka, M. A. Farr, A.-C. Uhlemann, P. C. Colombo and M. Yuzefpolkskaya, Abstract 18591: relationship between gut microbiota, inflammation and congestion among advanced heart failure patients, *Circulation*, 2017, **136**, A18591–A18591.
- 42 S. Liu, K. S. Joseph, W. Luo, L. J. Andrés, L. Sarka, V. D. H. Michiel, E. Jane, L. Ken, L. Julian and S. Reg, Effect of folic acid food fortification in Canada on congenital heart disease subtypes, *Circulation*, 2016, **134**, 647–655.
- 43 B. N. Francis, M. Salameh, R. Khamisy-Farah and R. Farah, Tetrahydrobiopterin (BH4): Targeting endothelial nitric oxide synthase as a potential therapy for pulmonary hypertension, *Cardiovasc. Ther.*, 2017, **36**, e12312.
- 44 I. Fleming and R. Busse, Endothelium-derived epoxyeicosatrienoic acids and vascular function, *Hypertension*, 2006, **47**, 629–633.
- 45 M. Nlr, N. M. Kouyoumdzian, A. Uceda, J. S. Del Mauro, M. Pandolfo, M. M. Gironacci, A. M. Puyó, J. E. Toblli, B. E. Fernández and M. R. Choi, Losartan prevents the imbalance between renal dopaminergic and renin angiotensin systems induced by fructose overload. L-dopa/dopamine index as new potential biomarker of renal dysfunction, *Metabolism*, 2018, **85**, 271–285.
- 46 N. P. Paynter, R. Balasubramanian, F. Giulianini, D. D. Wang, L. F. Tinker, S. Gopal, A. A. Deik, K. Bullock, K. A. Pierce, J. Scott, M. A. Martínez-González, R. Estruch, J. E. Manson, N. R. Cook, C. M. Albert, C. B. Clish and K. M. Rexrode, Metabolic predictors of incident coronary heart disease in women, *Circulation*, 2018, **137**, 841–853.
- 47 S. Fiorucci and E. Distrutti, Bile acid-activated receptors, intestinal microbiota, and the treatment of metabolic disorders, *Trends Mol. Med.*, 2015, **21**, 702–714.
- 48 V. H. V. Je, P. Veiga, C. Zhang, M. Derrien and L. Zhao, Impact of microbial transformation of food on health - from fermented foods to fermentation in the gastro-intestinal tract, *Curr. Opin. Biotechnol.*, 2011, **22**, 211–219.
- 49 J. L. SanchezAlonso, A. Bhargava, T. O'Hara, A. V. Glukhov, S. Schobesberger, N. Bhogal, M. B. Sikkel, C. Mansfield, Y. E. Korchev and A. R. Lyon, Microdomain-specific modulation of L-type calcium channels leads to triggered ventricular arrhythmia in heart failure, *Circ. Res.*, 2016, **119**, 944–955.
- 50 B. Mosca, O. Delbono, M. M. Laura, L. Bergamelli, Z. M. Wang, M. Vukcevic, R. Lopez, S. Treves, M. Nishi and H. Takeshima, Enhanced dihydropyridine receptor calcium channel activity restores muscle strength in JP45/CASQ1 double knockout mice, *Nat. Commun.*, 2013, **4**, 1541.
- 51 P. W. Cheng, Y. Y. Chen, W. H. Cheng, P. J. Lu, H. H. Chen, B. R. Chen, T. C. Yeh, G. C. Sun, M. Hsiao and C. J. Tseng,

- Wnt signaling regulates blood pressure by downregulating a GSK-3 $\beta$ -mediated pathway to enhance insulin signaling in the central nervous system, *Diabetes*, 2015, **64**, 3413–3424.
- 52 H. Ma, R. D. Groth, S. M. Cohen, J. F. Emery, B. Li, E. Hoedt, G. Zhang, T. A. Neubert and R. W. Tsien,  $\gamma$ CaMKII shuttles  $\text{Ca}^{2+}$ /CaM to the nucleus to trigger CREB phosphorylation and gene expression, *Cell*, 2014, **159**, 281–294.
- 53 Y. L. Tain, S. Leu, K. L. Wu, W. C. Lee and J. Y. Chan, Melatonin prevents maternal fructose intake-induced programmed hypertension in the offspring: roles of nitric oxide and arachidonic acid metabolites, *J. Pineal Res.*, 2014, **57**, 80–89.
- 54 A. Veillette, NK cell regulation by SLAM family receptors and SAP-related adapters, *Immunol. Rev.*, 2010, **214**, 22–34.
- 55 A.-M. Lompré, R. J. Hajjar, S. E. Harding, E. G. Kranias, M. J. Lohse and A. R. Marks,  $\text{Ca}^{2+}$  cycling and new therapeutic approaches for heart failure, *Circulation*, 2010, **121**, 822–830.
- 56 M. A. Lanaspa, M. Kuwabara, A. Andres-Hernando, N. Li, C. Cicerchi, T. Jensen, D. J. Orlicky, C. A. Roncal-Jimenez, T. Ishimoto, T. Nakagawa, B. Rodriguez-Iturbe, P. S. MacLean and R. J. Johnson, High salt intake causes leptin resistance and obesity in mice by stimulating endogenous fructose production and metabolism, *Proc. Natl. Acad. Sci. U. S. A.*, 2018, **115**, 3138–3143.
- 57 F. Yan, N. Li, J. Shi, H. Li, Y. Yue, W. Jiao, N. Wang, Y. Song, G. Huo and B. Li, *Lactobacillus acidophilus* alleviates type 2 diabetes by regulating hepatic glucose, lipid metabolism and gut microbiota in mice, *Food Funct.*, 2019, **10**, 5804–5815.
- 58 N. Qin, F. Yang, A. Li, E. Prifti, Y. Chen, L. Shao, J. Guo, C. E. Le, J. Yao and L. Wu, Alterations of the human gut microbiome in liver cirrhosis, *Nature*, 2014, **513**, 59–64.
- 59 J. D. Lewis, E. Z. Chen, R. N. Baldassano, A. R. Otley, A. M. Griffiths, D. Lee, K. Bittinger, A. Bailey, E. S. Friedman, C. Hoffmann, L. Albenberg, R. Sinha, C. Compher, E. Gilroy, L. Nessel, A. Grant, C. Chehoud, H. Li, G. D. Wu and F. D. Bushman, Inflammation, Antibiotics, and Diet as Environmental Stressors of the Gut Microbiome in Pediatric Crohn's Disease, *Cell Host Microbe*, 2015, **18**, 489–500.
- 60 I. Moreno-Indias, L. Sánchez-Alcoholado, P. Pérez-Martínez, C. Andrés-Lacueva, F. Cardona, F. Tinahones and M. I. Queipo-Ortuño, Red wine polyphenols modulate fecal microbiota and reduce markers of the metabolic syndrome in obese patients, *Food Funct.*, 2016, **7**, 1775–1787.
- 61 K. Kasahara, K. A. Krautkramer, E. Org, K. A. Romano, R. L. Kerby, E. I. Vivas, M. Mehrabian, J. M. Denu, F. Bäckhed, A. J. Lusis and F. E. Rey, Interactions between *Roseburia intestinalis* and diet modulate atherogenesis in a murine model, *Nat. Microbiol.*, 2018, **3**, 1461–1471.
- 62 G. Hajishengallis and R. J. Lamont, Dancing with the stars: how choreographed bacterial interactions dictate nosocomiality and give rise to keystone pathogens, accessory pathogens, and pathobionts, *Trends Microbiol.*, 2016, **24**, 477–489.
- 63 J. U. Scher, S. Andrew, R. S. Longman, S. Nicola, U. Carles, B. Craig, R. Tim, C. Vincenzo, E. G. Pamer and S. B. Abramson, Expansion of intestinal *Prevotella*, copro-correlates with enhanced susceptibility to arthritis, *eLife*, 2013, **2**, e01202.
- 64 Z. Jie, H. Xia, S.-L. Zhong, Q. Feng, S. Li, S. Liang, H. Zhong, Z. Liu, Y. Gao, H. Zhao, D. Zhang, Z. Su, Z. Fang, Z. Lan, J. Li, L. Xiao, J. Li, R. Li, X. Li, F. Li, H. Ren, Y. Huang, Y. Peng, G. Li, B. Wen, B. Dong, J.-Y. Chen, Q.-S. Geng, Z.-W. Zhang, H. Yang, J. Wang, J. Wang, X. Zhang, L. Madsen, S. Brix, G. Ning, X. Xu, X. Liu, Y. Hou, H. Jia, K. He and K. Kristiansen, The gut microbiome in atherosclerotic cardiovascular disease, *Nat. Commun.*, 2017, **8**, 845.
- 65 A. Jacobson, L. Lam, M. Rajendram, F. Tamburini, J. Honeycutt, T. Pham, W. Van Treuren, K. Pruss, S. R. Stabler, K. Lugo, D. M. Bouley, J. G. Vilches-Moure, M. Smith, J. L. Sonnenburg, A. S. Bhatt, K. C. Huang and D. Monack, A Gut Commensal-Produced Metabolite Mediates Colonization Resistance to *Salmonella*, *Infection, Cell Host Microbe*, 2018, **24**, 296–307.
- 66 O. Rådmark, O. Werz, D. Steinhilber and B. Samuelsson, 5-Lipoxygenase, a key enzyme for leukotriene biosynthesis in health and disease, *Biochim. Biophys. Acta, Mol. Cell Biol. Lipids*, 2015, **1851**, 331–339.
- 67 K. Chalupsky, D. Kračun, I. Kanchev, K. Bertram and A. Görlach, Folic acid promotes recycling of tetrahydrobiopterin and protects against hypoxia-induced pulmonary hypertension by recoupling endothelial nitric oxide synthase, *Antioxid. Redox Signaling*, 2015, **23**, 1076–1091.
- 68 F. Pluteanu, J. Heß, J. Plackic, Y. Nikanova, J. Preisenberger, A. Bukowska, U. Schotten, A. Rinne, M. C. Kienitz and M. K. H. Schäfer, Early subcellular  $\text{Ca}^{2+}$  remodelling and increased propensity for  $\text{Ca}^{2+}$  alternans in left atrial myocytes from hypertensive rats, *Cardiovasc. Res.*, 2015, **106**, 87–97.
- 69 H. Kesteloot, I. Tzoulaki, I. J. Brown, Q. Chan, A. Wijeyesekera, H. Ueshima, L. Zhao, A. R. Dyer, R. J. Unwin and J. Stamler, Relation of urinary calcium and magnesium excretion to blood pressure: the international study of macro- and micro-nutrients and blood pressure and the international cooperative study on salt, other factors, and blood pressure, *Am. J. Epidemiol.*, 2011, **174**, 44–51.
- 70 I. Bogeski and B. Niemeyer, Redox regulation of ion channels, *Antioxid. Redox Signaling*, 2014, **21**, 859–862.
- 71 J. E. Hall, Renal dysfunction, rather than nonrenal vascular dysfunction, mediates salt-induced hypertension, *Circulation*, 2016, **133**, 894–906.
- 72 X. Zheng, X. Li, M. Chen, P. Yang, X. Zhao, L. Zeng, Y. OuYang, Z. Yang and Z. Tian, The protective role of hawthorn fruit extract against high salt-induced hypertension in Dahl salt-sensitive rats: impact on oxidative stress and metabolic patterns, *Food Funct.*, 2019, **10**, 849–858.

- 73 N. R. Barbaro, J. D. Foss, D. O. Kryshtal, N. Tsyba, S. Kumaresan, L. Xiao, R. L. Mernaugh, H. A. Itani, R. Loperena, W. Chen, S. Dikalov, J. M. Titze, B. C. Knollmann, D. G. Harrison and A. Kirabo, Dendritic cell amiloride-sensitive channels mediate sodium-induced inflammation and hypertension, *Cell Rep.*, 2017, **21**, 1009–1020.
- 74 H. Lyu, X. Ji, Z. Zhou, M. Zhuang, Q. Yang, S. Jin, K. Cho and J. Wen, Protective effect of phycion on homocysteine-induced endothelial dysfunction via activation of PI3-kinase/Akt- and  $\text{Ca}^{2+}$ -eNOS-NO pathway, *J. Am. Coll. Cardiol.*, 2017, **70**, C12.
- 75 G. Yang, G. Istanas, S. Höges, M. Yakoub, U. Hendgen-Cotta, T. Rassaf, A. Rodriguez-Mateos, L. Hering, M. Grandoch and E. Mergia, Angiotensin-(1–7)-induced Mas receptor activation attenuates atherosclerosis through a nitric oxide-dependent mechanism in apolipoproteinE-KO mice, *Pflug. Arch. Eur. J. Physiol.*, 2018, **470**, 661–667.
- 76 T.-R. Wu, C.-S. Lin, C.-J. Chang, T.-L. Lin, J. Martel, Y.-F. Ko, D. M. Ojcius, C.-C. Lu, J. D. Young and H.-C. Lai, Gut commensal *Parabacteroides goldsteinii* plays a predominant role in the anti-obesity effects of polysaccharides isolated from *Hirsutella sinensis*, *Gut*, 2019, **68**, 248–262.
- 77 S. Yang, Y. Qu, H. Zhang, Z. Xue, T. Liu, L. Yang, L. Sun, Y. Zhou and Y. Fan, Hypoglycemic effects of polysaccharides from Gomphidiaceae rutilus fruiting bodies and their mechanisms, *Food Funct.*, 2020, **11**, 424–434.
- 78 F. F. Anhê, D. Roy, G. Pilon, S. Dudonné, S. Matamoros, T. V. Varin, C. Garofalo, Q. Moine, Y. Desjardins and E. Levy, A polyphenol-rich cranberry extract protects from diet-induced obesity, insulin resistance and intestinal inflammation in association with increased *Akkermansia*, spp. population in the gut microbiota of mice, *Gut*, 2015, **64**, 872–883.
- 79 C.-H. Peng, J.-J. Cheng, M.-H. Yu, D.-J. Chung, C.-N. Huang and C.-J. Wang, *Solanum nigrum* polyphenols reduce body weight and body fat by affecting adipocyte and lipid metabolism, *Food Funct.*, 2020, **11**, 483–492.
- 80 A. Rodriguez-Mateos, C. Rendeiro, T. Bergillos-Meca, S. Tabatabaee, T. W. George, C. Heiss and J. P. Spencer, Intake and time dependence of blueberry flavonoid-induced improvements in vascular function: a randomized, controlled, double-blind, crossover intervention study with mechanistic insights into biological activity, *Am. J. Clin. Nutr.*, 2013, **98**, 1179–1191.